Reducing NDT Effort by Coupled Monitoring and Simulation of Liquid Composite Molding Processes

Nico Liebers*, Dominic Bertling

Institute of Composite Structures and Adaptive Systems,
German Aerospace Center (DLR), Braunschweig, Germany
*corresponding author, E-mail: nico.liebers@dlr.de

Abstract

Liquid Composite Molding (LCM) is a manufacturing technique which could reduce material and process costs in comparison to the widely used prepreg processes. The raw materials are less expensive and easier to store and geometrical complex parts can be manufactured. But LCM requires more sophisticated process design due to its sensitivity to deviations in the raw materials or process setup. Gaps for example can lead to race tracking which often results in trapped gas inside of the component. Such gas inclusions can lead to porosity or even larger dry spots and thus an unusable part.

The DLR Institute of Composite Structures and Adaptive Systems developed flexible low cost ultrasonic sensors for LCM monitoring. The sensors do not require direct contact to the part and therefore do not affect the part surface or mold. Due to enhanced signal analysis not only the flowfront arrival can be detected, but also its flow speed. Further the moments of wetting of the mold surface and the infiltration through the part thickness can be distinguished. The sensor system is also able to perform cure monitoring including the detection of gelation and vitrification points.

These sensor inputs are coupled with a fast flow simulation where the model parameters are adapted to match the measurement by a sophisticated optimization algorithm. The most important model parameters are the permeability and gap sizes. By adapting the simulation the pointwise monitoring results are transformed into a 2.5-dimensional representation of the flowfront that enables the prediction of its further course. The results are used to detect possible gas inclusions and areas of high porosity. If none of these defects are detected the NDT process could be omitted. In the case of detected defects only these areas would have to be tested potentially.

1. Introduction

While fiber reinforced plastics possess excellent weight specific properties their high cost is preventing a broad application. On one hand the cost of raw materials is high and on the other hand the manufacturing process and the process development is expensive. Also the NDT of composite parts is very costly as in aeronautics all primary structure parts are inspected completely.

Liquid Composite Molding (LCM) is a manufacturing technique, for production of fiber reinforced composites, with the potential to reduce material and process costs in comparison to the widely used prepreg processes [1]. In contrast to prepregs (*pre*im*preg*nated), where the material supplier already impregnated the fibers with resin, in LCM the resin is injected into the dry fibers as part of the manufacturing process chain. The dry fiber semi finished products as well as the resins used for LCM are less expensive than prepreg materials. Also as prepregs have to be stored at usually $-18\ ^{\circ}C$, the storage of LCM raw materials is more cost effective. For example injection resins can be used where the resin and hardener components are stored separately at room temperature as the unmixed components cannot cure.

But the LCM process is also very challenging. The raw materials and the so called *preform* – the stack of oriented, cut and formed fiber layers – have high deviations in their properties. The relatively sensitive injection process to these deviations therefore leads to different filling patterns and possible defects.

A quick overview over the principle of LCM processes and their challenges is given in the next section. After this the non-invasive ultrasound-based method for LCM monitoring is presented and finally the enhancement of collected sensor values with a flow simulation is briefly described.

2. Liquid Composite Molding processes

Liquid Composite Molding is the process of impregnating dry fiber materials – or more precisely the cavities between the fibers – with a resin. The driving force is a pressure gradient between the cavity and the resin reservoir. The principle of this process is shown in Figure 1 for a closed mold process. In closed mold processes two rigid mold halves are used forming a defined cavity between them, where the fiber material is placed before closing the mold. In many cases the cavity is evacuated before starting the impregnation. This reduces the size of air pores in the final part and their probability, besides it increases the pressure gradient between the cavity and the resin reservoir.

When the resin inlet is opened the resin starts to flow through the resin line into the mold. As mentioned before the resin flow is driven by the pressure gradient between the resin inlet (injection pressure p_{inj}) and the cavity p_{vac}. If the pressure difference $p_{\text{inj}} - p_{\text{vac}}$ remains equal the flowfront

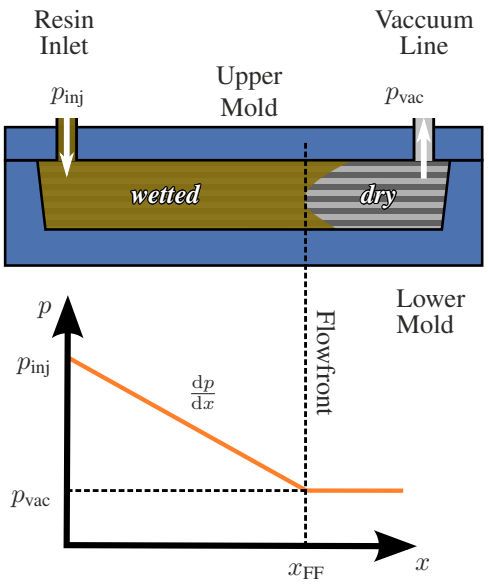

Figure 1: Liquid Composite Molding (LCM) process in closed mold with resin pressure distribution. The flowfront marks the interface between the dry and the impregnated fibers.

speed decreases as the pressure gradient is reduced over the growing flow length from the resin inlet to the flowfront position x_{FF}. The 1d volume-averaged flow velocity q_{xx} can be calculated by Darcy's Law, where K_{xx} is the fiber's permeability in x-direction and η the resin's viscosity [2].

$$q_x = \frac{dx}{dt} = -\frac{K_{xx}}{\eta} \cdot \frac{dp}{dx} \tag{1}$$

The resin viscosity decreases with temperature while it increases with the degree of cure. At higher degrees of cure the viscosity increases exponentially and the resin transits from a liquid to a gel. This is the so-called point of gelation and marks the theoretical limit for the molding process. The flow process stops much earlier, depending on the height of the pressure gradient.

In geometrical complex parts and parts with complex fiber layups the permeability varies over the part. Also other cavities like the gaps at the edges of fiber patches or at the outer edges of the part usually possess higher permeability where the resin flow can reach significantly higher speeds. This can lead to so-called *race tracking*, where the flowfront progresses much faster around the fiber material and finally meets at the vacuum line before the whole part is impregnated.

In Figure 2 the evolution of several flowfronts forming a dry spot is shown. This dry spot can only be filled if the pressure gradient suffices and the resin remains able to flow. As under real production conditions the vacuum pressure is not absolute zero, a volume of air is entrapped in the dry spot. With shrinking dry spot volume the gas pressure is increasing which leads to a smaller pressure gradient between the dry spot and the surrounding resin and thus to a reduced resin flow into the dry spot.

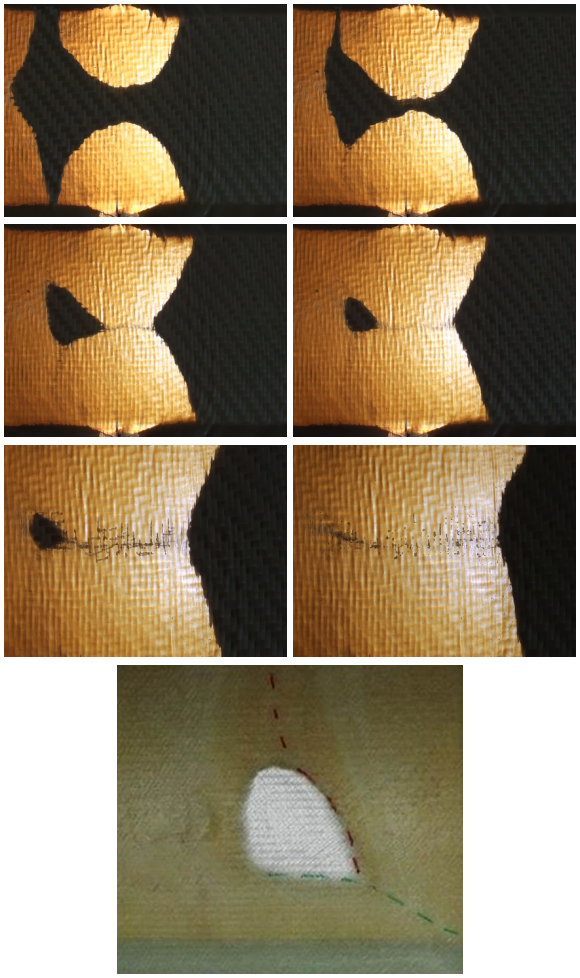

Figure 2: *First and second row*: Different flowfronts meet during infusion and trap gas
Third row: Resin flows into the dry spot and removal takes place as dispersion
Bottom: Remaining dry spot in cured glass fiber composite part

Depending of the size and the Darcy parameter (Equation 1) such a dry spot can remain and render a part unusable, as seen in the bottom picture of Figure 2. There are some measures to reduce the dry spot size or remove it completely. One is to "flush" the part to remain a pressure gradient and resin flow into the dry spot by letting both the resin and the vacuum line opened. The removal of the dry spot takes place as dispersion of the dry spot and removal of voids. Mobile voids are removed by reaching the flowfront, remaining stationary voids can dissolve into the resin completely. [3]

Another is to increase the pressure inside the mold with a closed vacuum line. First, the higher pressure leads to smaller dry spots due to compression of enclosed air. Second, the amount of dissolved gas in a liquid is proportional to its pressure (Henry's law) [4].

Normally both procedures are combined. After flushing the mold the vacuum line is closed and the injection pressure is increased.

3. Ultrasonic Flowfront Monitoring

In order to detect possible dry spots and to control the counter measures a flowfront monitoring system is required. There is a great number of sensor principles to detect the flowfront position. In open-mold processes instead of a rigid upper mold a vacuum membrane is used. The membrane is often a transparent polymer allowing the visual flowfront detection. But this is not possible in all cases, especially not for closed-mold technologies. Even with transparent membranes or mold halves only the upper flowfront surface can be obtained.

Apart of visual observation the flowfront detection can be realized amongst others by thermocouples [5], by thin metallic wires inside the fiber material either by reflection at the flowfront of electrical signals [6] or guided mechanical waves [7], in the fibers embedded piezoelectric sensors [8] and by measuring either the resin's electrical resistance [9] or its dielectric properties [10, 11]. But all these measurement principles require direct contact with the resin in order to detect the flowfront arrival or position. Either the sensors need to be embedded in the composite or into the mold. The sensor embedding is not always allowed and is hence limited in application. Mounting sensors into the mold risks the vacuum tightness of the mold and the sensors usually leave marks on the part surface. As this is usually a disadvantage, the sensors can only be placed at the border but not in the areas of interest.

The decisive advantage of ultrasonic or – more general – acoustic sensors is that no direct contact to the part is needed as the sound waves can be send through the mold wall. Also ultrasound sensors can be designed to sustain high temperatures [12] and pressure. At the DLR Institute of Composite Structures and Adaptive Systems ultrasonic sensors particularly well suited for LCM monitoring and data processing algorithms were developed. The sensors and the flowfront monitoring principles are described in the following sections.

3.1. Adapted Ultrasound Sensors

Most research on ultrasonic composite manufacture monitoring focuses on the resin cure [13, 14], but also for flowfront monitoring [15]. There are some studies to use ultrasound C-scan technique to track the impregnation [16, 15]. Stoven et al [17] developed a special ultrasound transducer for flow monitoring in thickness direction of the composite. In all these studies ultrasonic transducers are used which are either placed directly on the part surface or with a couplant on the outer mold wall.

The first method leads to markups and reduced mold tightness and the latter was found to be unstable under production conditions. In industrial composite manufacturing – especially in aeronautics – the used resins require elevated temperatures for impregnation and cure. These temperature differences were found to cause reduced coupling between the ultrasound transducer and mold wall and finally failure of the monitoring system. Even counter measures like alternative coupling materials and using a spring to maintain contact pressure against the mold wall could not effectively solve this issue. Only when piezoelectric discs were adhesively mounted onto the mold and used as transducer a stable signal during temperature changes could be achieved [18, 19].

The principle of mold mounted piezoelectric elements for ultrasonic composite monitoring is shown in Figure 3 and compared to conventional transducers. The conventional transducers consist also of a piezoelectric element which is placed inside a housing on a delay line and is usually damped for a short broad bandwidth signal. Compared to the bare piezoelectric there is one additional interface between the delay line and the mold wall. At this interface part of the signal energy is reflected leading to reduced transmitted amplitude and additional echoes when using an pulse-echo-configuration. With the new method the mold wall is used as a delay line and the first echo returning to the sensor originates from the mold-laminate-interface simplifying signal analysis.

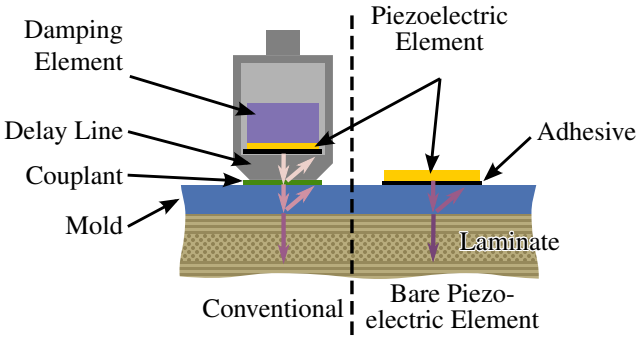

Figure 3: Principle of conventional ultrasound transducer and bare piezoelectric element as sensors for composite process monitoring

In addition to a clearer and stronger signal the novel sensor configuration is significantly less expensive and therefore the sensor cost is not the bottleneck for the number of sensors. Due to its minimal space requirement it is easy to integrate into new molds as well as to retrofit into existing molds with relatively low effort.

3.2. Flowfront Detection

In order to detect the flowfront arrival at the sensor location the pulse-echo as well as the transmission mode can be used. In Figure 4 both principles are shown as a scheme with the plots of the respective amplitude evolution. In the case of pulse-echo-method when the resin has not yet arrived at the sensor location (a) the sound signal is reflected completely. When the interface between mold and part is starting to get impregnated (b) the reflected amplitude decreases until the whole surface is filled (c) and remains constant (d), as the reflection factor at the wetted surface R_{wet} is lower than at the dry surface R_{dry}. The latter can be con-

sidered to be $|R_{\text{dry}}| \approx 1$. The normalized amplitude of the reflected pulse-echo signal $\bar{A}_{\text{PE}}$ hence depends on the ratio of the wetted surface S_{wet} and the total reflection surface area S_{sensor}:

$$\bar{A}_{\text{PE}} = \frac{A_{\text{PE}}}{A_{\text{PE, dry}}} = 1 - \frac{S_{\text{wet}}}{S_{\text{sensor}}} \cdot \left(1 - \frac{R_{\text{wet}}}{R_{\text{dry}}}\right) \tag{2}$$

With $|R_{\text{dry}}| = 1$:

$$\bar{A}_{\text{PE}} = 1 - \frac{S_{\text{wet}}}{S_{\text{sensor}}} \cdot (1 - |R_{\text{wet}}|) \tag{3}$$

The reflection factor R depends on the impedances Z_1 and Z_2 of the two materials at the interface, which themselves depend on their density ϱ and sound velocity c:

$$R = \frac{Z_2 - Z_1}{Z_2 + Z_1} \quad \text{with } Z_i = c_i \cdot \varrho_i \tag{4}$$

In the case that the $Z_2 > Z_1$ the reflection factor is negative, which means that the reflected signal is phase shifted by π.

The amount to which the amplitude drops is proportional to the reflection factor after wetting R_{wet}:

$$\bar{A}_{\text{PE, wet}} = \frac{A_{\text{PE, wet}}}{A_{\text{PE, dry}}} = \frac{R_{\text{wet}}}{R_{\text{dry}}} \tag{5}$$

which depends on the mold material's impedance and is usually much higher (hence $R < 0$). For aluminum molds the amplitude drops by approximately 18 %, while for steel molds the drop is only 7 %. For composite molds the drop is much higher as the impedance is closer to the impedance of the liquid resin. For metallic molds the signal change can be enhanced using multiple reflections. Extending Equation 5 by the number of reflections n yields:

$$\bar{A}_{\text{PE, wet}} = \left(\frac{R_{\text{wet}}}{R_{\text{dry}}}\right)^n \tag{6}$$

Using the transmission mode the amplitude only changes when the volume between the transmitter and receiver is "bridged" by resin (c) as the sound signal cannot propagate through the dry fibers and vacuum. Until the whole volume is impregnated the amplitude is increasing (d). The final transmission amplitude might be reached long after the resin has passed due to gas bubbles near the flowfront.

Combining the two pulse-echo-signals from each mold and the transmission signal the shape of the flowfront over the thickness can be derived as outlined in Figure 5. In most cases the resin flow speed is higher at the mold-fiber interface than inside the fiber stack. One scenario is a wedge shape, where the second pulse-echo amplitude plot reaches a plateau at the same time as the transmission signal. This is also the case for the example above in Figure 4. The delay between the two pulse-echo signals is a measure for the angle of the wedge.

If the transmission amplitude reaches the plateau after the two pulse-echo amplitudes then the flowfront is most probably U-shaped (right hand side in Figure 5). This U-shaped flowfront bears the risk of dry spot inclusions when the flowfront at the mold interfaces meet for example at the border of the cavity.

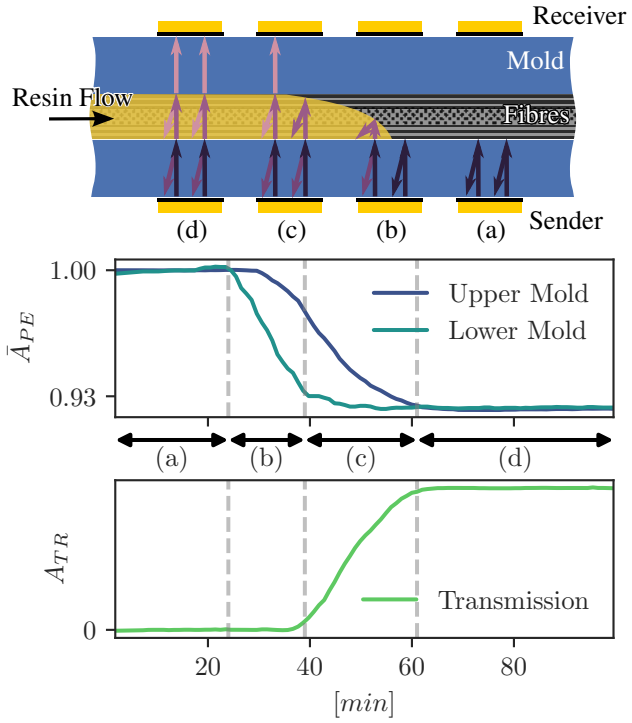

Figure 4: Principle of flowfront detection by pulse-echo and transmission modes. The plots show the amplitude evolution of the three signals (pulse-echo signals from each mold halve and the transmission signal) during passing flowfront from an experiment with a steel mold. For clearer pulse-echo amplitude calculation the fourth echo was used.

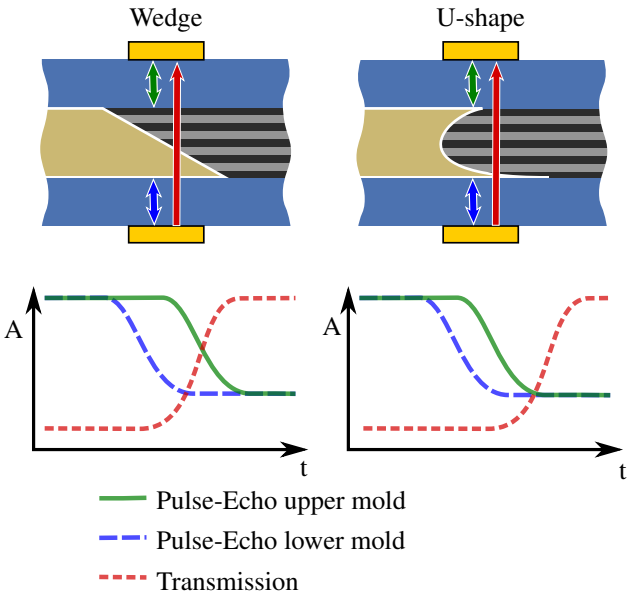

Figure 5: Estimation of the flowfront shape from the amplitude evolution of the two pulse-echo and the transmission signals

3.3. Flowfront Speed Measurement

The detection of the flowfront arrival at the sensor location is a very valuable input for the production design, optimization and control. But even when using a large number of sensors the fill pattern during the LCM process cannot be completely reconstructed in some cases. Therefore the speed of the flowfront when passing the sensor location could be beneficial.

According to Equation 2 in Section 3.2 the pulse-echo amplitude decreases while the interface area over the sensor subsection is wetted. Hence the flowfront speed v_{FF} is:

$$v_{\text{FF}} = \frac{D_{\text{sensor}}}{t_{\text{Fill}}} \tag{7}$$

With the sensor's diameter D_{sensor} and the time t_{Fill} to fill the sensor's cross section.

But this is only true if the transmitter emitted a homogeneous sound pressure field. Real sound transmitter generate a complex inhomogeneous pressure field. In Figure 6 there are two examples of the sound intensity distribution for two different mold thicknesses. The distribution was calculated by a ray tracing method developed in [19] and is not described in detail in this paper, but the result is shown to illustrate the problem. The ray tracing method is mimicing the Huygens–Fresnel principle, which states that from each point of the surface of the sound emitter a spherical wavelet is transmitted. The sum of these wavelets form the wavefront. The wavelets are emitted from the sensor surface, propagating through the mold, reflected from the mold surface and arrive back at the sensor surface after traveling through the mold again. As the spherical wavelet surface is increasing with the travel length its intensity is decreasing. In function of the reflection location (in front or behind the flowfront) and the incident angle the reflection factor must be calculated. Also the wavelets return with a different phase to the sensor depending on their path length.

The flowfront is drawn as a dashed red line in Figure 6 and positioned exactly at the middle of the sensor. On the left hand side the distribution shows the sound intensity for a relatively thin and on the right hand side for a thicker mold wall. Comparing the two shows inhomogeneous but very different patterns and the thicker the mold the more the sound intensity is focused on the center. This effect has to be taken into account for a precise flowfront speed measurement.

Not only the mold thickness, but also the mold material, sensor size and sound frequency play a major role. For every variation of these parameters either a correction factor has to be identified. The factor can either be determined experimentally or by a calculation model. The ray tracing model has not yet been verified sufficiently which is planned for future work.

The flowfront speed measurement was verified by a experimental setup with a transparent mold (PMMA), on which the sensors were mounted and the flowfront position was monitored by a video camera and automated image processing (Figure 7). The experiments were conducted

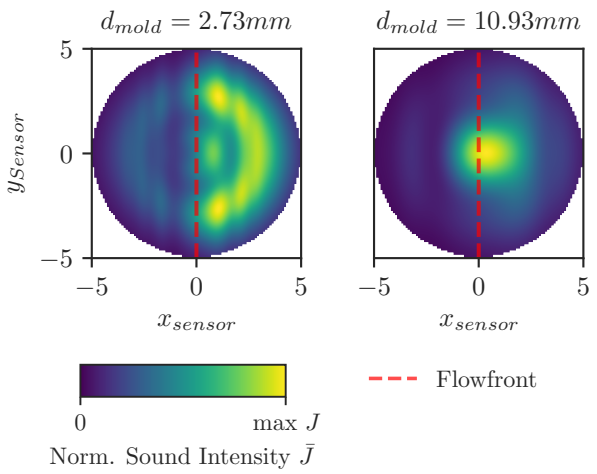

Figure 6: Calculated sound intensity distribution over the sensor cross section of the reflected signal for different mold thicknesses with the current flowfront position (dashed red line, middle axis of sensor). Mold material is PMMA.

with a silicone oil mixed with a colorant to simplify the video analysis. The results are considered to be comparable to a resin. The reflection amplitude was measured with an interval of about $\triangle t \approx 0.16\ s$ for each of the 10 sensors and the flow speed was in the range of $5.5 \leq v_{\text{FF}}\left[\frac{mm}{min}\right] \leq 14$.

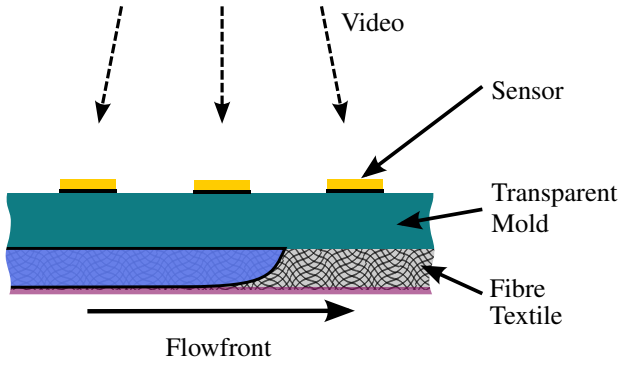

Figure 7: Experimental setup

Figure 8 shows the result of the amplitude evolution exemplary for one sensor. In order to obtain the duration of the amplitude drop different algorithms were tested. One was to use amplitude thresholds and use the time difference between both.

Another considered algorithm was to use parametric curves to fit the measured values, where one of the fitted parameters is a measure for the amplitude drop duration. As the shape of the temporal derivative of the amplitude resembles a Gaussian function it was chosen for the curve fitting method.

$$P_{\text{Gauss}} = \gamma \cdot \exp\left(-\frac{(t-\mu)^2}{2\sigma^2}\right) \tag{8}$$

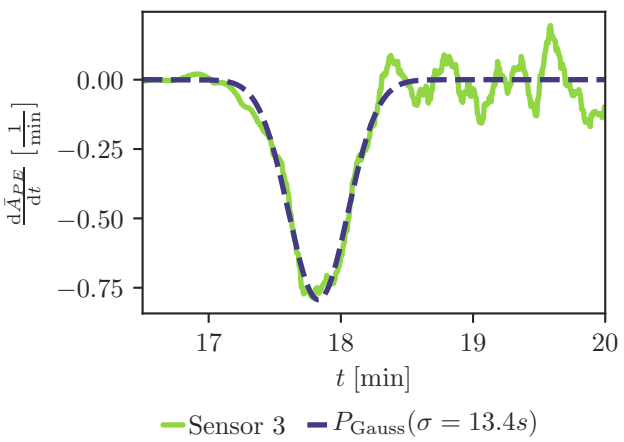

Figure 8: Derivative of the reflection amplitude or flowfront speed measurement with thresholds and fitted curve P_{Gauss}. Noise was removed by moving average with a window size of 5.

The parameter σ is then used to derive the flowfront speed. To calculate the derivative from the noise-prone data the Savitzky-Golay algrotithm was used [20]. As it can be observed in Figure 8 the curve fit is very close to the measured amplitude.

To calculate the flowfront speed from the obtained amplitude drop durations either by thresholds or by fitting the Gaussian function need to be corrected by a factor κ which also takes into account the effective sensor area. Expanding Equation 7 with the factor leads to:

$$v_{\mathrm{FF}} = \kappa \frac{D_{\mathrm{sensor}}}{t_{\mathrm{Fill}}} \tag{9}$$

The factor needs to be obtained either experimentally or by a calculation model. The results of the experiment were used to calculate the correctional factors by correlating with the flowfront speed from video analysis. The correlation is shown in Figure 9, where the correctional factor is already applied. The curve fitting method by the Gaussian function scores the best correlation as it can be taken form Table 1. Both methods attain a relatively high correlation coefficient, but the curve fitting method achieves a lower standard deviation of $0.44\ \frac{mm}{min}$.

Table 1: Flowfront speed measurement results

	Threshold	Curve Fit P_{Gauss}
Correction Factor κ	3.81	6.08
Standard Deviation	$0.76\frac{mm}{min}$	$0.44\ \frac{mm}{min}$
Correlation Coeff.	0.973	0.994

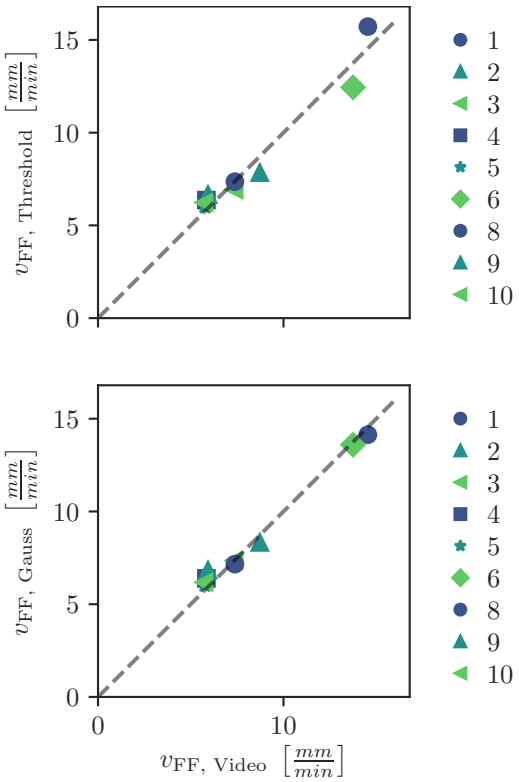

Figure 9: Correlation of flowfront speed measurement by analysing the amplitude drop and video processing (data of Sensor 7 was not exploitable)

3.4. Cure Monitoring

Besides the flowfront the ultrasonic sensors can also be used for cure monitoring. As the resin reacts chemically its mechanical modules are increasing which lead to a growing sound velocity. A typical sound velocity development during the isothermal cure of an epoxy resin is shown in Figure 10. While the velocity forms an ”s-shape” and is monotonically growing with an asymptotic end. Hence the sound velocity is a reliable indicator for the degree of cure, but also depends on the temperature. With increasing temperature the sound velocity is decreasing.

The amplitude has a characteristic local minimum during cure. This amplitude minimum is suspected to be caused by the vitrification process [13]. At the vitrification point the resin’s mechanical properties raise strongly as the molecule mobility is reduced and therefore the cure process comes almost to an end. At this point the composite part can be demolded or the cure temperature has to be increased to enhance the degree of cure. Another important point is the gellation, where the resin transits from a liquid to a gel as the molecular network spans the whole resin (but not all chemical links are connected). At this point the resin is not able to flow anymore but it can transmit forces.

Both transition points can be derived from the sound velocity trace. Figure 11 shows the results of ultrasound measurements inside a rheometer. The sensors were installed on the disks of the rheometer and acquired the transmis-

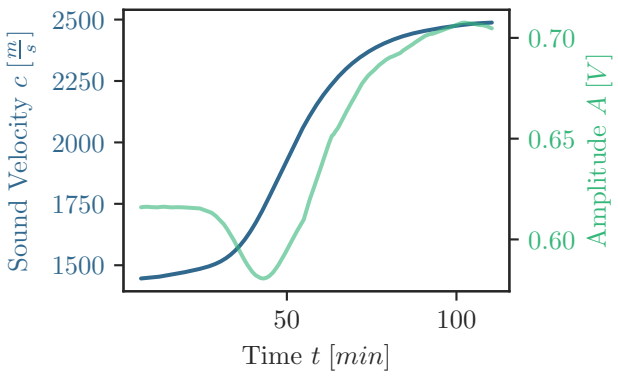

Figure 10: Typical sound velocity and amplitude evolution during isothermal cure

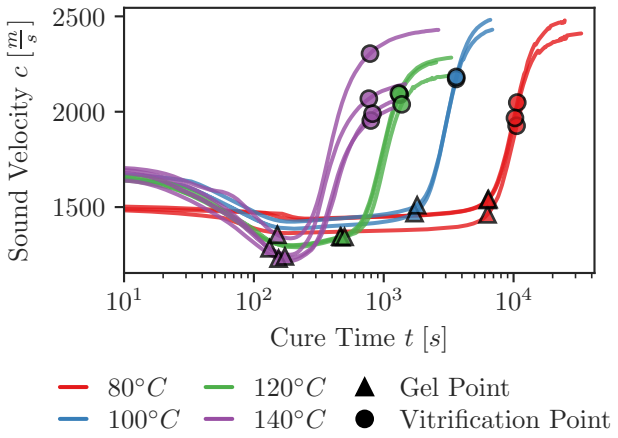

Figure 11: Correlation of sound velocity with gel and vitrification points obtained by simultaneous measurement in rheometer

sion signal during cure at different cure temperatures. The rheometer is an established method to obtain the gellation and vitrification points from the complex shear modulus. Onto the sound velocity traces these points are drawn as markers. The gellation (△) occurs for all experiments at the same characteristic point, where the sound velocity curves start to increase significantly (the "onset"). Some authors [14, 13] have proposed a tangent method to reliably obtain this point.

The position of the vitrification point (○) is depending on the cure temperature. While at high cure temperatures the point is on the "offset" of the curves, at lower temperature the points move toward the inflection point of the s-shaped curves. It has been shown, that from calibration measurements such as in Figure 11 these points can be detected by neural networks at the latest a upon their occurrence [19]. This would overcome the disadvantage of the tangent methods which depend on the curve after the gellation or vitrification points have already occured. The neural networks also showed better results than the unprecise detection of the vitrification by tangent method.

4. Flow Simulation

The high complexity of the production of composite parts leads to costly preliminary tests or scrap parts during production start-up. Depending on the component and production technology, deviations from the planned flow pattern also occur during production. Production-related variations in the draped, dry reinforcement structures are one reason for unexpected deviations. In addition to the documentation of the manufacturing process and the reduction of the quality assurance effort, the DLR developed a *R*esin *I*mpreg*n*ation *Syst*e*m* (*RINSE*) to detect production deviations online in order to be able to initiate corrective measures as soon as possible.

For this purpose, RINSE is built as a platform that connects several third party software with own code. The System searches for a flow simulation that fits best to the real world data measured by the ultrasound sensors for each individual component. The flow simulation model parameters are adapted to match the local measurements by a sophisticated optimization algorithm. The result of the comparison allows statements to be made about the ongoing process and enables the derivation of component-specific correction measures as mentioned in chapter 2. It also enables the localization and valuation of defects during production.

The chance of defects is quantified by a numerical simulation that describes the dissolution behavior of dry areas in the pressure field of LCM processes. Due to the low flow velocities and porous nature of the fiber, two-phase simulation of air-resin system is based on the pressure-saturation approach formulated using Darcy's law. The relative permeability model takes into account the influence on the flow of each phase in the presence of the other phase. The model shows good agreement with experimental test results at reasonable computing times and allows the derivation of corrective measures for the resolution of dry spots. [21]

5. Conclusions

Low cost ultrasonic sensors have been presented, which can be mounted effortless onto the outer side of molds and allow a high number of sensors. The sensors can obtain the flowfront arrival time at the sensor position, but also the flowfront shape and furthermore its flow speed. Also the resin cure and gellation and vitrification points can be monitored. The sensor results are fed into a fast flow simulation and an optimization algorithm adapts the model parameters to fit the data. Hence possible deviations such as local permeability of the textile can be taken into account. The simulation results are analyzed for possible dry spots.

Acknowledgement

This work was supported by the German Federal Ministry for Economic Affairs and Energy on the basis of a decision by the German Bundestag (Grant 20W1521E) under research program of 'LuFo V-2'.

References

[1] M. G. Bader, "Selection of composite materials and manufacturing routes for cost-effective performance," *Composites Part A: Applied Science and Manufacturing*, vol. 33, no. 7, pp. 913–934, 2002.

[2] H. Darcy, "Les fontaines publiques de la ville de Dijon. Exposition et application des principes à suivre et des formules à employer dans les questions de distribution d'eau," 1856.

[3] D. Bertling, R. Kaps, and E. Mulugeta, "Analysis of dry-spot behavior in the pressure field of a liquid composite molding process," *CEAS Aeronautical Journal*, vol. 7, no. 4, pp. 577–585, aug 2016.

[4] W. Henry, "III. experiments on the quantity of gases absorbed by water, at different temperatures, and under different pressures," *Philosophical Transactions of the Royal Society of London*, vol. 93, pp. 29–274, jan 1803.

[5] G. Tuncol, M. Danisman, A. Kaynar, and E. M. Sozer, "Constraints on monitoring resin flow in the resin transfer molding (RTM) process by using thermocouple sensors," *Composites Part A: Applied Science and Manufacturing*, vol. 38, no. 5, pp. 1363–1386, 2007.

[6] G. Pandey, H. Deffor, E. T. Thostenson, and D. Heider, "Smart tooling with integrated time domain reflectometry sensing line for non-invasive flow and cure monitoring during composites manufacturing," *Composites Part A: Applied Science and Manufacturing*, vol. 47, pp. 102–108, 2013.

[7] K. Visvanathan and K. Balasubramaniam, "Ultrasonic torsional guided wave sensor for flow front monitoring inside molds," *The Review of scientific instruments*, vol. 78, no. 1, p. 15110, 2007.

[8] X. Wang, L. Ye, Y.-W. Mai, C. Ehlers, C. Kissinger, and M. Neitzel, "Potential of Piezoelectric Elements in the Monitoring of Composite Manufacturing Process," *Journal of Intelligent Material Systems and Structures*, vol. 8, no. 12, pp. 1073–1078, 1997.

[9] N. Pantelelis and E. Bistekos, "Process monitoring and control for the production of CFRP components," Seattle, USA, 2010.

[10] M. Kazilas and Cranfield University, *Acquisition and Interpretation of Dielectric Data for Thermoset Cure Monitoring*. Cranfield University, 2003.

[11] A. McIlhagger, D. Brown, and B. Hill, "The development of a dielectric system for the on-line cure monitoring of the resin transfer moulding process," *Composites Part A: Applied Science and Manufacturing*, vol. 31, no. 12, pp. 1373–1381, 2000.

[12] R. Kazys, A. Voleisis, R. Sliteris, L. Mazeika, R. van Nieuwenhove, P. Kupschus, and H. A. Abderrahim, "High temperature ultrasonic transducers for imaging and measurements in a liquid Pb/Bi eutectic alloy," *IEEE Transactions on Ultrasonics, Ferroelectrics and Frequency Control*, vol. 52, no. 4, pp. 525–537, 2005.

[13] J. McHugh, *Ultrasound technique for the dynamic mechanical analysis (DMA) of polymers*. Berlin: Bundesanstalt für Materialforschung und -prüfung (BAM), 2008.

[14] F. Lionetto and A. Maffezzoli, "Monitoring the Cure State of Thermosetting Resins by Ultrasound," *Materials*, vol. 6, no. 9, pp. 3783–3804, 2013.

[15] T. Luthy, *Three-dimensional permeability measurements based on direct current and ultrasound monitoring techniques*. Diss., Technische Wissenschaften ETH Zürich, Nr. 15050, 2003, 2003.

[16] H. L. Liu, X.-C. Tu, J. O. Lee, H.-B. Kim, and W. R. Hwang, "Visualization of resin impregnation through opaque reinforcement textiles during the vacuum-assisted resin transfer molding process using ultrasound," *Journal of Composite Materials*, vol. 48, no. 9, pp. 1113–1120, 2014.

[17] T. Stöven, F. Weyrauch, P. Mitschang, and M. Neitzel, "Continuous monitoring of three-dimensional resin flow through a fibre preform," *Composites Part A: Applied Science and Manufacturing*, vol. 34, no. 6, pp. 475–480, 2003.

[18] N. Liebers, "Autoclave Infusion of Aerospace Ribs Based on Process Monitoring and Control by Ultrasound Sensors," Copenhagen, 23.07.2015.

[19] ——, "Ultraschallsensorgeführte Infusions- und Aushärteprozesse für Faserverbundkunststoffe," Dissertation, TU Braunschweig, Braunschweig, 2018. [Online]. Available: https://elib.dlr.de/121155/

[20] A. Savitzky and M. J. E. Golay, "Smoothing and Differentiation of Data by Simplified Least Squares Procedures," *Analytical Chemistry*, vol. 36, no. 8, pp. 1627–1639, 1964.

[21] D. Bertling and N. Liebers, "Analysis and simulation of dry-spot behavior in liquid composite molding," in *FPCM14, Lulea, Sweden*, 2018.